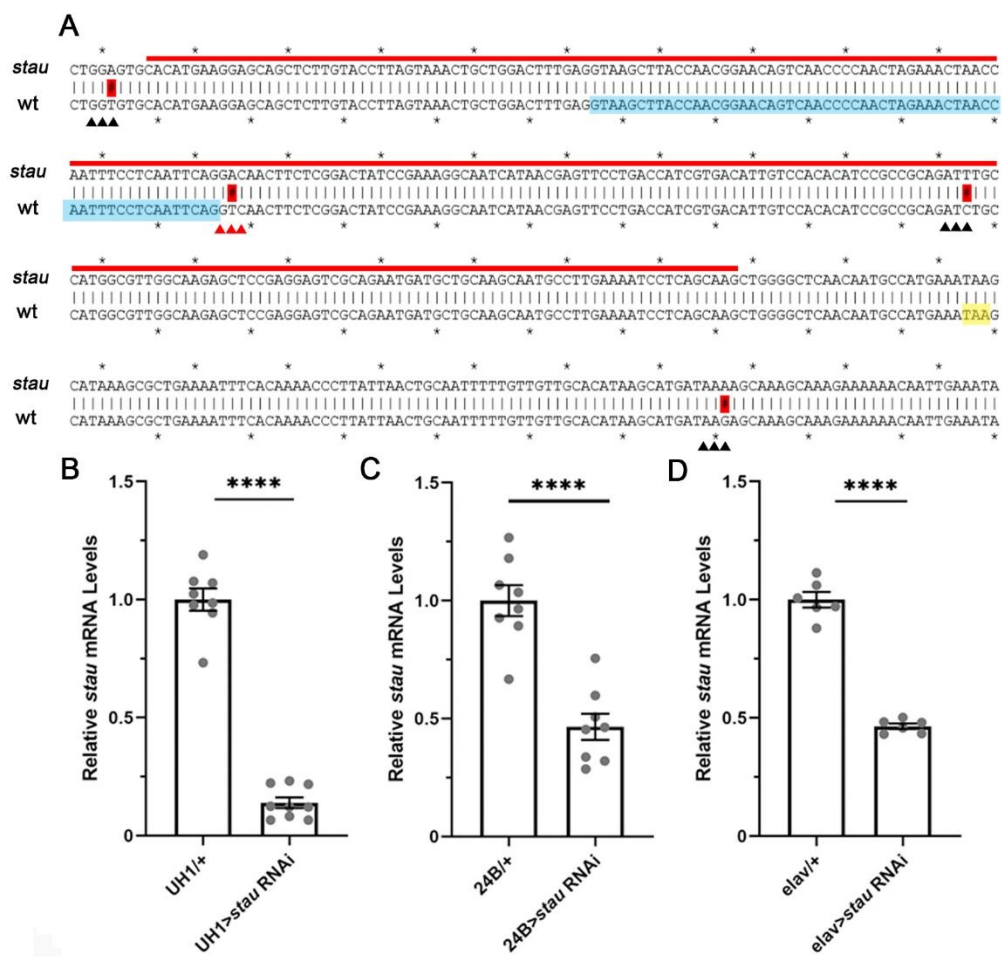


Fig. S1. Song et al.

**Fig. S1. Mutant *staufen*^{HL} sequence and *staufen* RNAi knock-down efficiency**

(A) The *staufen*^{HL} mutant sequence compared to wildtype sequence (<http://flybase.org/>). The double strand RNA-binding domain 5 (dsRBD5, red underline) contains a single intron (blue shading). In the mutant, silent mutant codon (black triangles) and nonsense mutant codon (red triangles) with mutated nucleotide (red shading) upstream of the stop codon (yellow shading). **(B-D)** Larval qPCR measurements of *staufen* RNAi efficiency with ubiquitous UH1-Gal4 **(B)**, muscle-targeted 24B-Gal4 **(C)** and neuron-targeted *elav*-Gal4 **(D)**. Significance is indicated at p<0.0001 (****) based on student's t-tests.

Fig. S2. Song et al.

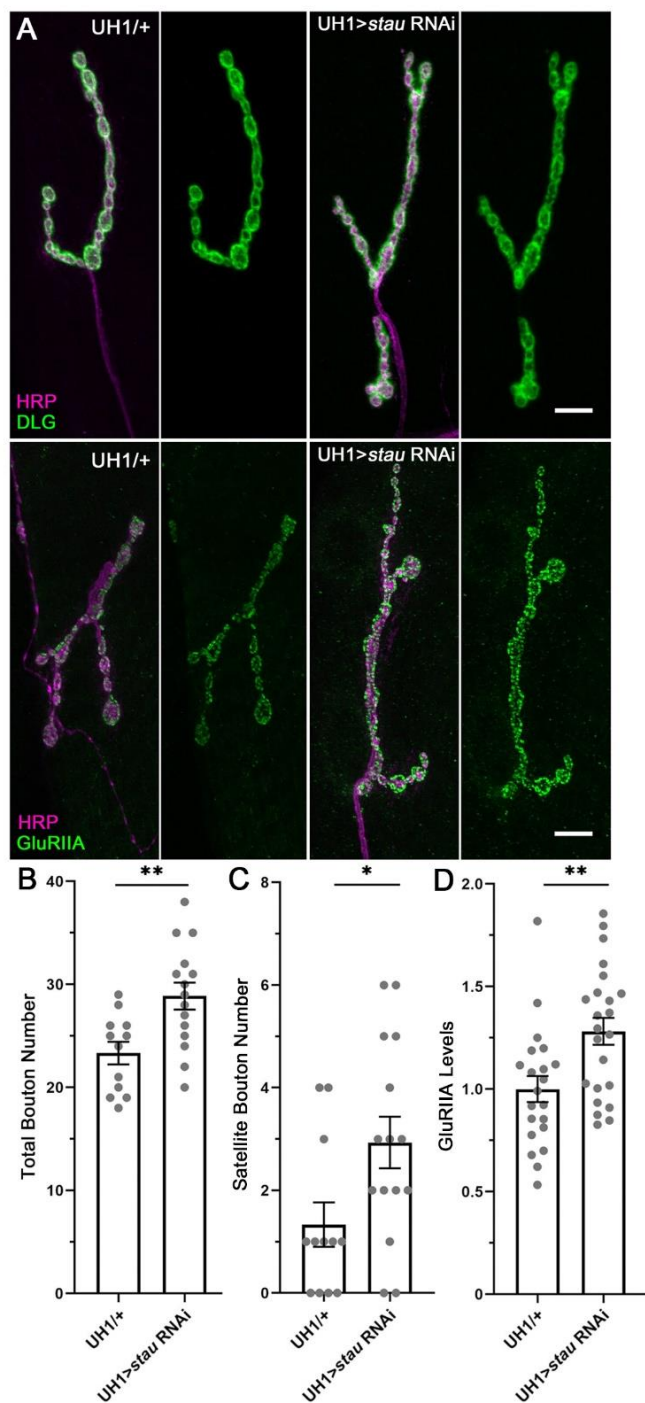


Fig. S2. *staufen* RNAi increases synaptic bouton formation and GluRIIA levels
Larval NMJ structure and GluRIIA levels compared between transgenic control (UH1^{+/+}) and *staufen* knockdown (UH1>*stau* RNAi). **(A)** Double labeling for presynaptic anti-HRP (magenta) and either postsynaptic DLG (green, top) or GluRIIA (green, bottom). Scale bar: 10 μm. Quantification of total synaptic bouton **(B)** and satellite bouton **(C)** number. **(D)** Quantification of GluRIIA fluorescence intensity normalized to genetic background control. Significance is indicated at p<0.05 (*) and p<0.01 (**) based on student's t-tests.

Fig. S3. Song et al.

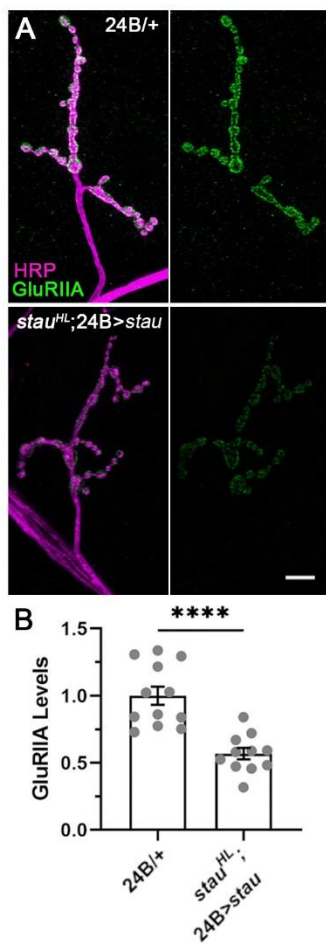


Fig. S3. Postsynaptic muscle-targeted *staufen* rescue decreases GluRIIA levels

Larval NMJs labeled for GluRIIA comparing transgenic control (24B/+) with postsynaptic muscle UAS-*staufen* expression in *staufen*^{HL} (*stau*^{HL}) homozygous mutant background (*stau*^{HL}; 24B>*stau*). **(A)** Double labeling for both presynaptic anti-HRP (magenta) and anti-GluRIIA (green) in the 24B-Gal4/+ control (top) and muscle *staufen* rescue in the *stau*^{HL} mutant (bottom). GluRIIA labeling alone is shown on the right for both genotypes. Scale bar: 10 μ m. **(B)** Quantification of the normalized GluRIIA fluorescence intensity. Significance is indicated at p<0.0001 (****).

Fig. S4. Song et al.

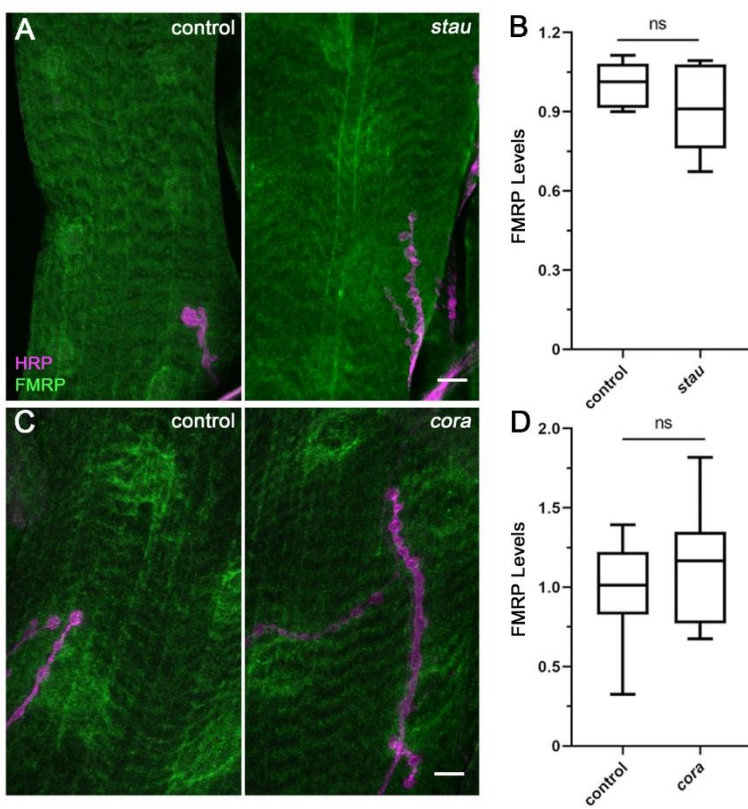


Fig. S4. Neither *staufen* and *coracle* mutants affect muscle FMRP levels

Larval muscles labeled for FMRP comparing genetic background control (w^{1118}) with *staufen* ($stauf^{HL}$) and *coracle* (cor^{14}) mutants. **(A)** Double labeling for anti-FMRP (green) and synaptic anti-HRP (magenta) in control versus *staufen* mutant. Scale bar: 10 μ m. **(B)** Quantification of FMRP levels shows no significant (ns) change. **(C)** Double labeling for FMRP (green) + HRP (magenta) in control versus *coracle* mutant. Scale bar: 10 μ m. **(D)** Quantification of FMRP levels shows no significant (ns) change.

Fig. S5. Song et al.

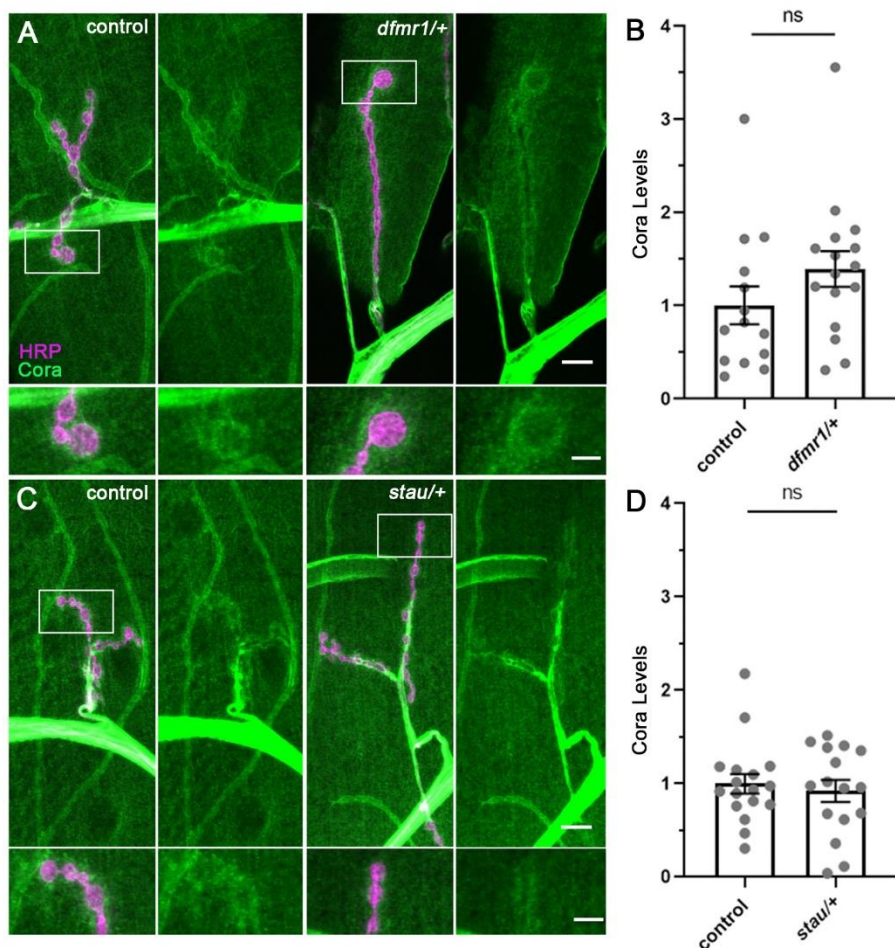
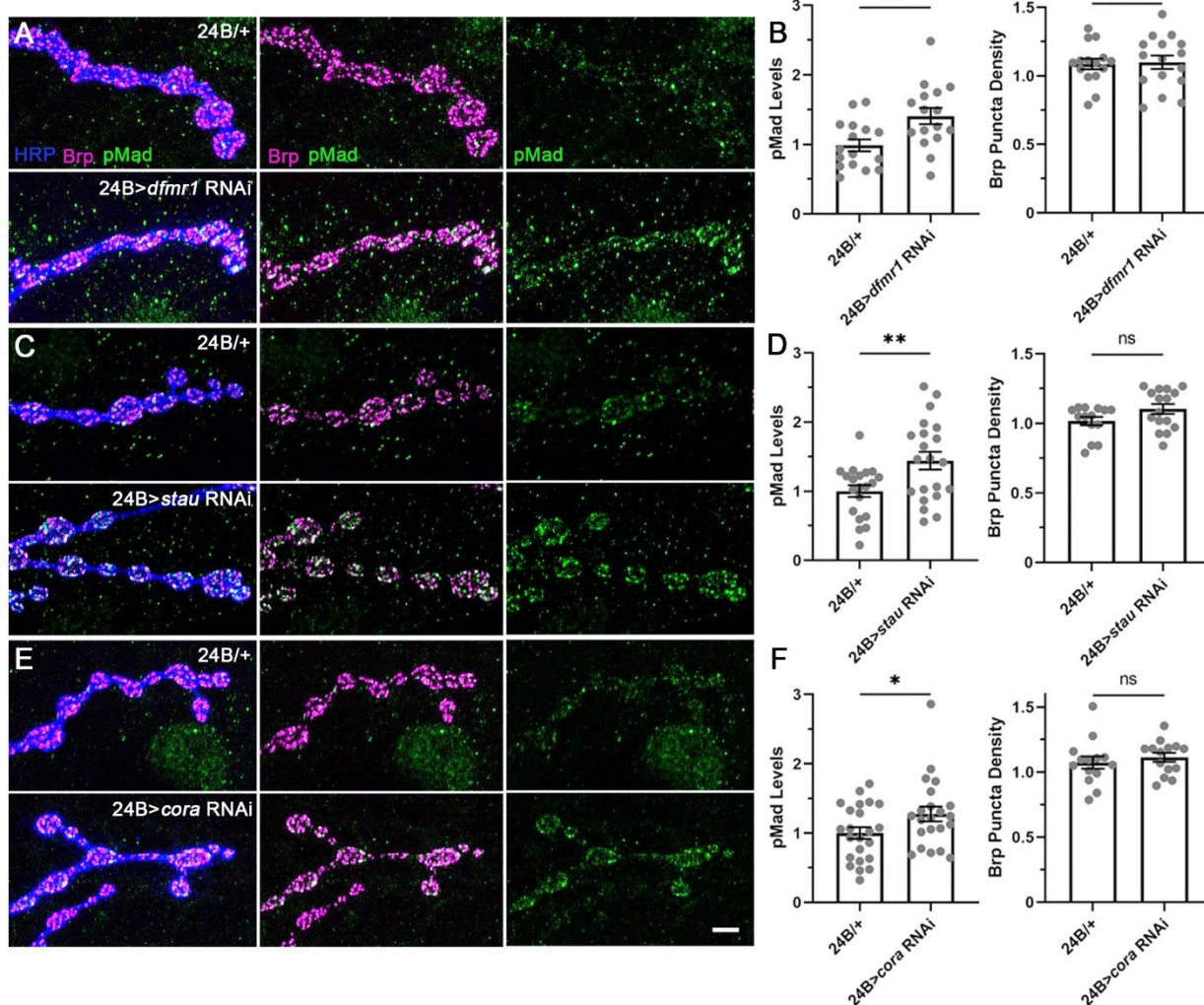


Fig. S5. Heterozygous *dfmr1*+/+ and *staufen*+/+ do not affect Coracle levels

Larval NMJs labeled for Coracle in controls (w^{1118}) compared to *dfmr1* (*dfmr1*^{50M}+/+) and *staufen* (*stauf*^{HL}+/+) heterozygotes. Top rows show full muscle 4 NMJs (scale bar: 10 μ m) with white-boxed regions shown magnified below (scale bar: 5 μ m). **(A)** Double labeling for presynaptic HRP (magenta) and Coracle (Cora, green) in control versus *dfmr1* heterozygote. **(B)** Postsynaptic Coracle levels normalized to control show no significant (ns) change. **(C)** NMJ Coracle labeling shown in control versus *staufen* heterozygote. **(D)** Postsynaptic Coracle levels normalized to control show no significant (ns) change.

Fig. S6. Song et al.

**Fig. S6. Postsynaptic FMRP, Staufen and Coracle all restrict pMad signaling**

Larval NMJs triple-labeled for HRP (blue), Brp (magenta) and pMad (green) in muscle driver controls (24B⁺, top rows) and with *dfmr1* (24B>*dfmr1* RNAi), *staufen* (24B>*stau* RNAi) and *coracle* (24B>*cora* RNAi) knockdown. **(A)** Representative images of *dfmr1* postsynaptic RNAi. **(B)** Quantification of normalized pMad fluorescent intensity (left) and Brp active zone density (right). **(C)** Representative images of muscle-targeted *staufen* knockdown. **(D)** Quantification of pMad levels and Brp active zone density. **(E)** Images of *coracle* postsynaptic RNAi. Scale bar: 5 μ m. **(F)** Quantification of presynaptic pMad levels and Brp active zone density. Significance is indicated at $p<0.05$ (*), $p<0.01$ (**) and $p>0.05$ (not significant; ns) based on student's *t*-tests.

Table S1. Transgenic UAS lines used in this study.

Line	Provider	Reference
UAS- <i>stau</i> RNAi	VDRC 106645	(Landskron et al. 2018)
UAS- <i>stau</i> RNAi	BDSC 31247	(Mahoney et al., 2016)
UAS- <i>cora</i> RNAi	BDSC 51845	(Jiang et al., 2019)
UAS- <i>dfmr1</i> RNAi	BDSC 35200	(Flockhart et al., 2006)
UAS-myc- <i>cora</i>	Fehon Lab	(Ward IV et al., 1998)
UAS- <i>stau</i> -GFP	Ramaswami Lab	(Barbee et al., 2006)
UAS-YFP- <i>dfmr1</i>	Zarnescu Lab	(Cziko et al., 2009)

Table S2. Primers used in this study.

Primer (forward)	Sequence	Primer (reverse)	Sequence
Staufen	GTAAACTGCTGGACTTGAGGTC	Staufen	GCAGGCATCATTCTGCGACTCC
GAPDH	CGTTCATGCCACCACCGCTA	GAPDH	CACGTCCATCACGCCACAA
Tubulin	ATTTACCCAGCACCACAAGTGT	Tubulin	GGCGATTGAGATTCATGTAGGTGG
Futsch	TTCCTGGATATTGCAGGACGG	Futsch	CTCGGGCAATGTGTGCCATA
Coracle	AAGAACAAAGAAGGAGAAGGATGC	Coracle	CATTAACAGCCGCTCTGCAG
Pal1	ACGACTGGGGCAAGAACTTTTT	Pal1	CGTAGGATATGCCGGAGAAGG